

Supporting Information

Palladium Doped 1T-Phase Molybdenum Disulfide-Black Phosphorene Two-Dimensional Van der Waals Heterostructure for Visible-light Enhanced Electrocatalytic Hydrogen Evolution

Xiancheng Song,^{a,‡} Bin Li,^{b,‡} Wenchao Peng,^b Chi Wang,^a Kai Li,^c Yuanzhi Zhu^{a,*} and Yi, Mei^{a,*}

^a Faculty of Chemical Engineering, Yunnan Provincial Key Laboratory of Energy Saving in Phosphorus Chemical Engineering and New Phosphorus Materials, Kunming University of Science and Technology, Kunming 650500, Yunnan, China

^b School of Chemical Engineering and Technology, State Key Laboratory of Chemical Engineering, Collaborative Innovation Center of Chemical Science and Engineering, Tianjin University, Tianjin 300072, China

^c Faculty of Environmental Science & Engineering, Kunming University of Science & Technology, Kunming, 650500, China

*Corresponding author.

E-mail address: yuanzhi_zhu@kust.edu.cn

1. Experimental

1.1 Materials

The N, N-dimethylformamide (DMF, purity > 99.5%), Nafion solution (5 wt.%), ethanol (purity > 99.9%), tetrabutylammonium bromide (TBAB, purity > 99%), bulk molybdenum sulfide (< 2 μm, purity > 99.5%), palladium acetate (Pd(OAc)₂), N-butyllithium solution (2.5 M in hexanes), tin(IV) iodide (purity > 95%), tin (purity >99.5%), phosphorus red (purity > 99.999%), and Poly(diallyldimethylammonium chloride) solution (PDDA, 20 wt.% in water solution) were purchased from Aladdin Reagent (Shanghai) Co., Ltd.

1.2 Sample preparation

Synthesis of 1T-MoS₂: The 1T-MoS₂ nanosheets were prepared by Li intercalation/exfoliation

method. 0.5 g MoS₂ powders were reacted with 5 mL butyllithium at 65 °C for 10 h under N₂ atmosphere. The obtained Li-intercalated bulk MoS₂ powders were washed by hexane to remove excessive butyllithium and then exfoliated via the reaction between the intercalated Li with water. The obtained 1T-MoS₂ dispersion was further treated by centrifugation at 3000 rpm and 8000 rpm to remove the unexfoliated flakes and too small nanosheets, respectively, and then centrifuged several times at 12 000 rpm for 30 min until the pH is nearly neutral.

Synthesis of bulk BP: 500 mg of red phosphorus, 25 mg of Sn, and 15 mg of SnI₄ were sealed in an evacuated quartz tube. The tube was placed horizontally in a muffle furnace, and heated at 550 °C for 15 h with a heating ramp rate of 2 °C min⁻¹, followed by cooling down to 300 °C with a rate of 0.3 °C min⁻¹, then followed by natural cooling to room temperature, and the product was washed by 0.01 M HCl solution, water, and ethanol to remove the residual impurities.

Preparation of 2H-MoS₂: 0.2606 g of ammonium molybdate tetrahydrate ((NH₄)₆Mo₇O₂₄·4H₂O) and 0.5175 g of thiourea (CH₄N₂S) were dissolved in 35 ml H₂O and sonicated for 30 min to form a homogenous solution. Then the solution was transferred into a 50 ml Teflon-lined stainless-steel autoclave and heated to 200 °C for 20 h. The obtained precipitate was washed with deionized water for several times by centrifugation.

Preparation of Pd-2H-MoS₂: 40 mg 2H-MoS₂ and 80ml H₂O were added into a N₂-filled Shrek tube, then the as-prepared Pd(OAc)₂ solution (1 wt.% Pd in H₂O) was added according to the needed mass ratio of MoS₂:Pd. The mixture was stirred at 60 °C for 12 h to obtain the Pd-2H-MoS₂. The product was purified by centrifugation several times with water and then diluted to 0.2 mg mL⁻¹ for the next-step.

1.3 DFT Calculation Methods

The models were computed with density functional theory (DFT) using projected augmented wave method^[1] as implemented in the Vienna ab initio Simulation Package (VASP) code.^[2] The generalized gradient approximation (GGA) of Perdew-Burke-Ernzerhof (PBE) is used for the exchange-correlation

potential.^[3] Plane-wave basis set was used with an energy cutoff of 400 eV. The convergence criterion for electronic structure iteration was set to be 1×10^{-5} eV and structural optimization would be terminated until all forces were smaller than $0.01 \text{ eV}/\text{\AA}$, all the atoms were relaxed. The DFT-D3 method was applied to correct the van-der Waals interaction.^[4] The charge transfer was analyzed by calculating the charge density using the Bader charge analysis method.^[5,6] Vacuum slab was set to be 15 \AA to avoid interactions between adjacent layers, k-meshes was set as $1 \times 1 \times 1$ in this work.

The adsorption free energy can be defined as:

$$\Delta G_{H^*} = \Delta E + \Delta ZPE - T\Delta S$$

Where ΔE , ΔZPE , ΔS represent the adsorption energy of H atom, difference of zero-point energy and entropy of adsorbed H atom and free hydrogen molecule. The temperature was 298 K.

The adsorption energy is defined as:

$$\Delta E = E_{slab+H^*} - E_{slab} - \frac{1}{2}E_{H_2}$$

Where E_{slab+H^*} , E_{slab} , E_{H_2} represent the total energy of catalyst surface and adsorbed H atom, the energy of catalyst surface and the energy of hydrogen molecule.

2. Additional Information of Experimental Analysis

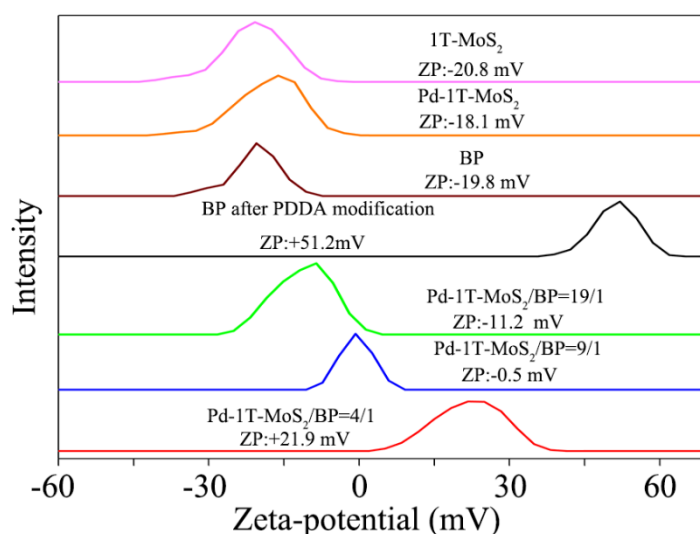


Figure S1. Zeta-potential results of dispersions of 1T-MoS₂, Pd-1T-MoS₂, BP, PDDA-modified BP,

Pd-1T-MoS₂/BP=19/1, Pd-1T-MoS₂/BP=9/1, and Pd-1T-MoS₂/BP=4/1, respectively. The Pd-1T-MoS₂ has a negative zeta potential of -18.1 mV, and the PDDA-modified BP nanosheet has a positive zeta potential of $+51.2$ mV, which indicates that the two nanosheets can be hybridized by electrostatic self-assembly. When the mass ratio of Pd-1T-MoS₂:BP is 9:1, the zeta potential of the obtained sample was closed to electric neutrality (-0.5 mV).

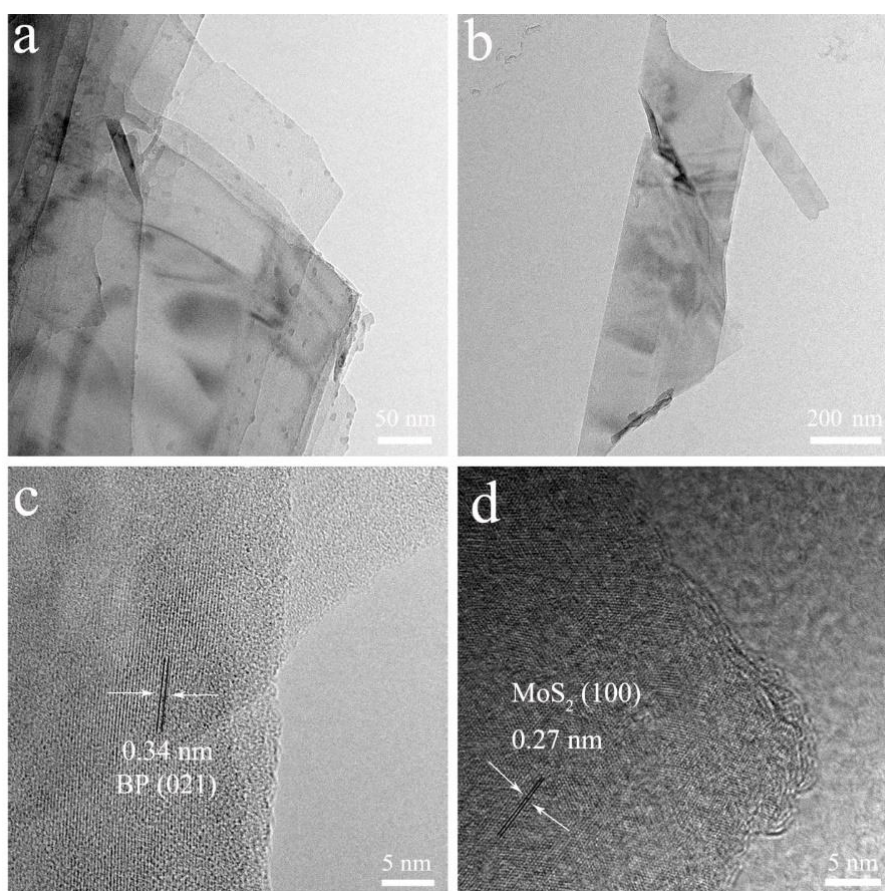


Figure S2. TEM images of (a) BP nanosheet and (b) Pd-1T-MoS₂. (c) HRTEM images of (c) BP nanosheets and (d) Pd-1T-MoS₂.

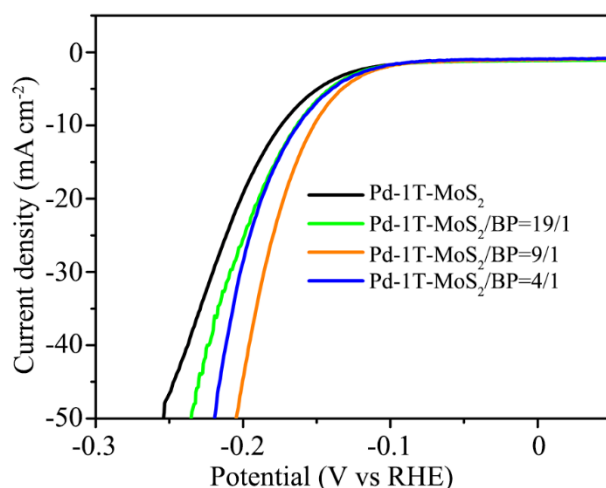


Figure S3. LSV for various Pd-1T-MoS₂/BP samples composed of different mass ratios of Pd-1T-MoS₂ and BP. As shown in Figure S3 and Figure S1, when the mass ratio of Pd-1T-MoS₂:BP is 9:1, the obtained sample exhibited the best HER performance and the zeta potential of the obtained sample was closed to electric neutrality (−0.5 mV).

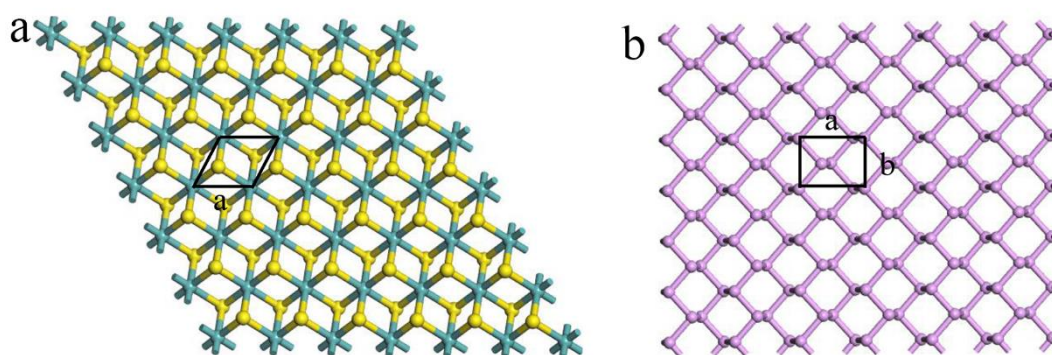


Figure S4. (a) Metal 1T phases MoS₂ nanosheets with a hexagonal unit cell, which belongs to space group R3M (No.160), the lattice parameter: $a = 0.32$ nm. (b) BP nanosheet with an orthorhombic unit cell, which belongs to space group Cmca (No. 64), the lattice parameters: $a=0.33$ nm, $b=1.05$ nm. For an approximate calculation, the ideal structures of a MoS₂ and BP were used to estimate the area balance between the Pd-1T-MoS₂ and PDDA-BP ($a \times a \times \sin 120^\circ \times N_A$ for Pd-1T-MoS₂ or $a \times b \times N_A$ for BP), where N_A is the Avogadro's number, $a \times a \times \sin 120^\circ$ and $a \times b$ are the in-plane unit cell area of MoS₂ and BP respectively. The mass ratio between monolayer MoS₂ (m-MoS₂) and monolayer BP (m-

BP) is: $m\text{-MoS}_2/m\text{-BP} = M(\text{MoS}_2)/(a \times a \times \sin 120^\circ \times N_A) / \{4M(\text{BP})/a \times b \times N_A\} = \sim 2.2$. Based on AFM results, the thickness of Pd-1T-MoS₂ and BP are 2–5 and 3–5 layers, respectively. Accordingly, for the formation of alternatively stacked 2D superlattices, the optimized $m(\text{Pd-1T-MoS}_2)/m(\text{BP})$ value should fall into the range of 0.88 to 3.6. This result suggests that the more ordered superlattice structure is not formed, which may be attributed to the mismatch of the lateral sizes of Pd-1T-MoS₂ and BP nanosheets.

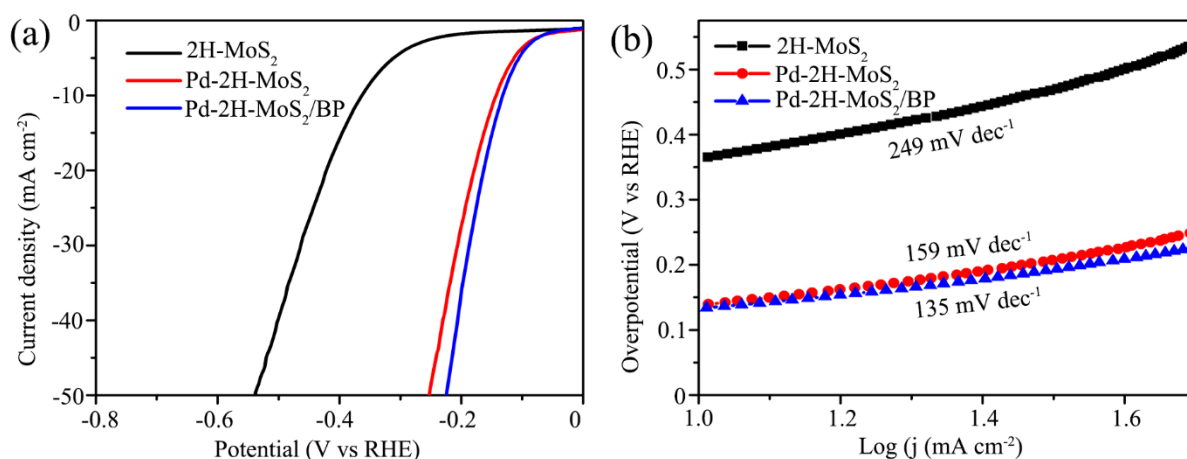


Figure S5. Polarization curves (a) and Tafel slop (b) of 2H-MoS₂, Pd-doped 2H-MoS₂ (Pd-2H-MoS₂) and the heterostructure (Pd-2H-MoS₂/BP) composed of Pd-2H-MoS₂P and BP nanosheets. In order to reveal the influence of contact area of heterointerface on the HER performance, the control sample composed of hydrothermally synthesized Pd-2H-MoS₂ with relatively amorphous structure was prepared for comparison. Although the Pd-2H-MoS₂ exhibited good HER performance, the Pd-2H-MoS₂/BP composite exhibited less improvement when composed with that of Pd-1T-MoS₂/BP in Figure 3. For example, Pd-1T-MoS₂/BP exhibited a 51 mV of decrease in overpotential at a current density of 50 mA cm⁻² and a Tafel slop of 86 mV dec⁻¹. However, the Pd-1T-MoS₂/BP only exhibited a 28 mV of decrease in overpotential at a current density of 50 mA cm⁻² and a Tafel slop of 135 mV dec⁻¹.

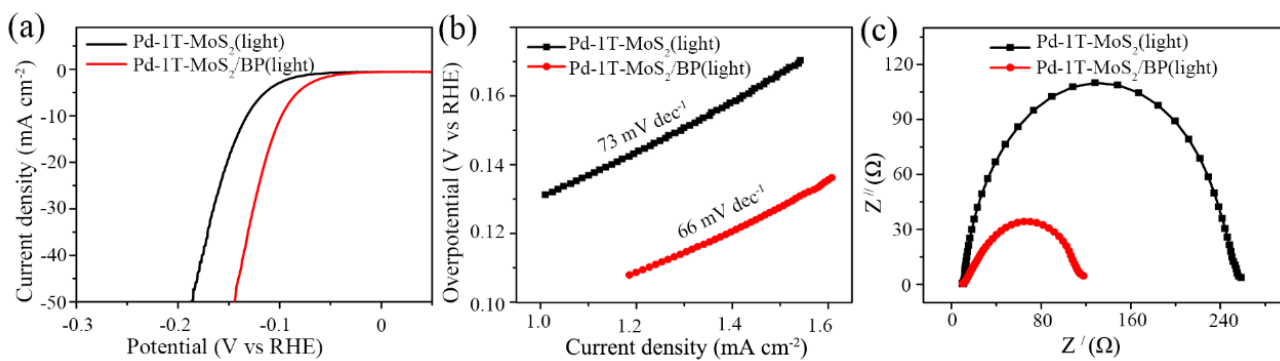


Figure S6. (a) Polarization curves of the Pd-1T-MoS₂, Pd-1T-MoS₂/BP electrode under light conditions. (b) Tafel plots of Pd-1T-MoS₂ and Pd-1T-MoS₂/BP; (c) EIS spectra over the frequency range from 1000 kHz to 0.01 Hz at $\eta=100$ mV.

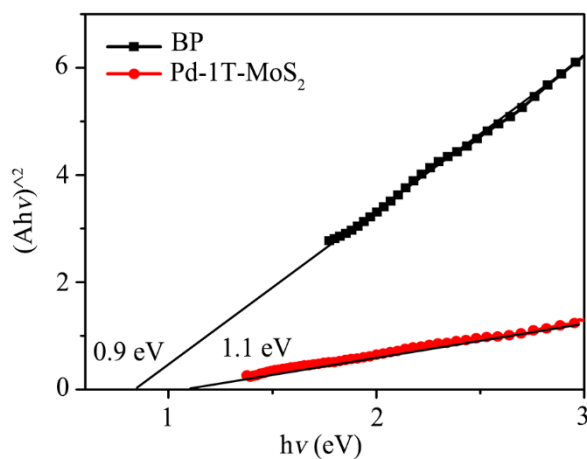


Figure S7. The Kubelka-Munk plot vs photon energy for BP and Pd-1T-MoS₂.

Table S1. The DFT calculated E_{slab+H^*} , E_{slab} , and ΔG_{H^*} .

	E_{slab+H^*} / eV	E_{slab} / eV	ΔG_{H^*} / eV
Pd-1T MoS ₂ /BP	-1208.6344	-1205.1385	0.0935
Pd-1T MoS ₂	-773.4136	-769.7236	-0.0965
1T MoS ₂	-782.1931	-778.7894	0.1935
BP	-434.4478	-431.6804	0.8335